Chemical Geology 420 (2016) 213–230

Contents lists available at ScienceDirect

Chemical Geology

journal homepage: www.elsevier.com/locate/chemgeo

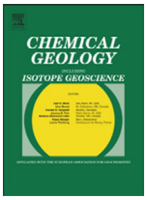

The structure of haplobasaltic glasses investigated using X-ray absorption near edge structure (XANES) spectroscopy at the Si, Al, Mg, and O *K*-edges and Ca, Si, and Al $L_{2,3}$-edges

Benjamin J.A. Moulton [a,*], Grant S. Henderson [a], Camille Sonneville [b], Cedrick O'Shaughnessy [a], Lucia Zuin [c], Tom Regier [c], Dominique de Ligny [d]

[a] *Dept. of Earth Sciences, University of Toronto, 22 Russell St., Toronto, ON M5S 3B1, Canada*
[b] *Ecole Normale Supérieure de Cachan, 61 Avenue du Président Wilson, 94235 Cachan Cedex, France*
[c] *Canadian Light Source Inc., University of Saskatchewan, 44 Innovation Boulevard, Saskatoon, SK S7N 2V3, Canada*
[d] *Dept. Werkstoffwissenschaften, Lehrstuhl für Glas und Keramik, Universität Erlangen-Nürnberg, Martensstr. 5, D-91058 Erlangen, Germany*

ARTICLE INFO

Article history:
Received 23 June 2015
Received in revised form 8 October 2015
Accepted 16 November 2015
Available online 19 November 2015

Keywords:
Haplobasalt
Anorthite
Diopside
X-ray absorption near-edge structure
Glass structure
Melts

ABSTRACT

X-ray absorption near-edge structure (XANES) spectroscopy has been used to investigate the local structural environments around each of the elements within the haplobasaltic system. The XANES results reveal both, linear changes in Ca, O and Si whereas non-linear changes are also observed for Si as well as Al and Mg. Unexpectedly, both Si and Al spectra show complex edge structure that varies non-linearly across the join. The Si $L_{2,3}$-edge results suggest that the Si environment in An100 is very similar to that in crystalline anorthite whereas the Di100 and diopside spectra show large offsets. The L_3 and L_2 peaks display a linear behavior whereas peak B of the Si $L_{2,3}$ spectra displays a non-linear behavior displaying a maximum position at the Di40 and Di100 compositions and decreasing in between. We estimate the Si—O bond length from shift in the peak B position which suggests a change in bond length between 1.58 and 1.66 Å across the join. The Al *K*-edge spectra suggests that there is a constant decrease in the inter-tetrahedral angle as Al is added. The local Mg environment displays non-linear changes in intensity and for compositions with An content greater than Di40 it appears that $^{[4]}$Mg plays an important role whereas $^{[5]}$Mg is dominant in diopside-rich melts, though octahedral coordinated Mg cannot be ruled out. The oxygen environment appears similar to crystalline anorthite in the haplobasaltic system. Calcium is present in highly distorted sites that are dominantly $^{[7]}$Ca in anorthite-rich glasses whereas $^{[8]}$Ca is more important in diopside-rich glasses. These results provide additional independent constraints on the atomic structure of haplobasaltic silicate melts and highlight the need for further investigation into the relationships between network formers, modifiers and the oxygen to which they are bound.

1. Introduction

The simplified haplobasaltic system remains an archetype model used to understand the properties and structure of mafic silicate melts (Bowen, 1915; Russell and Giordano, 2005; Giordano et al., 2008b). This is true for two main reasons. First, this system contains the elements: Ca, Mg, Si, Al and O which are the main constituents of basaltic melts and constitute typically more than 80 wt.% of whole rock chemical analysis (e.g. Class and Lehnert, 2012). Second, the Di–An join covers a greater range of polymerization than typically found in natural melts, from tholeiitic basalts (NBO/T = 0.83) to typical rhyolites (NBO/T = 0.03) (Mysen and Richet, 2005; Giordano et al., 2009). The simplified haplobasaltic system is composed of the end-member compositions $CaMgSi_2O_6$ (Di) (crystalline diopside) and $CaAl_2Si_2O_8$ (An) (crystalline anorthite) (Bowen, 1915). The An end-member is typically thought of as completely polymerized (NBO/T = 0) whereas Di is considered quite depolymerized (NBO/T = 2) (Mysen et al., 1982). As a result this system has had broad application as a starting point for understanding silicate melts and has been extensively studied for most properties at ambient conditions (Mysen et al., 1980; Dunn, 1982; Scarfe et al., 1983; McMillan, 1984; Richet and Bottinga, 1984; Shimizu and Kushiro, 1984; Taniguchi and Murase, 1987; Navrotsky et al., 1990; Neuville and Richet, 1991; Secco et al., 1991; Knoche et al., 1992; Taniguchi, 1992; Askarpour et al., 1993; Toplis and Richet, 2000; Mysen and Richet, 2005; Getson and Whittington, 2007; Giordano et al., 2008b), and references therein). One consistent finding of these studies is that some properties change in a non-linear way (e.g. Scarfe et al., 1983; Taniguchi and Murase, 1987). While the properties of the end members are well established, the intermediate mixtures are much less studied and show contrasting behavior depending on which side of the eutectic composition ($Di_{64}An_{36}$) your sample lies

---

* Corresponding author.
E-mail address: bja.moulton@utoronto.ca (B.J.A. Moulton).

http://dx.doi.org/10.1016/j.chemgeo.2015.11.016
0009-2541/

(e.g. Taniguchi and Murase, 1987; Taniguchi, 1989; Navrotsky et al., 1990; Knoche et al., 1992).

Our understanding of the physical properties of silicate melts has evolved contemporaneously with structural studies that have tried to establish causal mechanisms that explain variations in the bulk properties of these melts (e.g. Mysen and Richet, 2005; Giordano et al., 2009, and references therein). In fact, Harrison et al. (2013) have argued that understanding the causal relationships between chemical structure, at various scales, and physical properties are a fundamental area for progress in geoscience research. The haplobasaltic system has been the subject of extensive structural studies (e.g. Mysen, 2003; Kuryaeva, 2009) largely using Raman (Mysen et al., 1980; McMillan, 1984; Matson et al., 1986; Sykes and Scarfe, 1990; Daniel et al., 1995; McMillan and Wolf, 1995), infrared (Taniguchi and Murase, 1987; McMillan and Wolf, 1995), nuclear magnetic resonance (NMR) (Stebbins and Xu, 1997; Allwardt and Stebbins, 2004; Xue and Kanzaki, 2008; Hiet et al., 2009) and X-ray absorption spectroscopies, as well as X-ray (Taylor and Brown, 1979; Drewitt et al., 2015) and neutron diffraction (Cormier and Cuello, 2013). However, two aspects of this research limit the insight necessary to extrapolate these results to natural systems. Firstly, no technique alone fully describes the melt structure. Therefore, multi-spectroscopic approaches have become the standard (e.g. Neuville et al., 2004b), each technique providing important data and constraints on the possible interpretations. Secondly, the above studies typically report results for end-member compositions and/or the eutectic composition. The eutectic composition, $Di_{64}An_{36}$ (where subscripts denote the molar proportions of the end-member diopside and anorthite compositions), is used as a first-order model for the natural basalt system (e.g. Asimow and Ahrens, 2010). As a result of the structural and physiochemical complexity of the anorthite end-member (Ai and Lange, 2008) and known anomalies in the diopside system (e.g. Reid et al., 2003) it is unclear if there is a single structural underpinning or a combination of structures required to best model the eutectic composition. Therefore, the better constrained the haplobasaltic system is at ambient conditions, the more testable are hypotheses regarding the behavior of this system at conditions relevant to the Earth.

The goal of this study is to constrain the local structure of each element in the haplobasaltic system and evaluate these structures relative to previous studies. This study investigates the haplobasaltic system in mixtures of Di and An at 20 mol. % intervals using a multi-edge X-ray absorption near-edge structure (XANES) approach. We report samples in terms of their $CaMgSi_2O_6$ content, DiX, such that the "X" represents the mol. % of the diopside component and the anorthite component equals 100-"X" ($Di80 = Di_{80}An_{20}$). $CaAl_2Si_2O_8$ glass is labeled An100. XANES spectroscopy is used to inspect each element in this system in order to resolve its local atomic environment (e.g. Henderson et al., 2014). Finally, we discuss the implications of these structural changes in their ability to explain linear and nonlinear changes in certain structural properties.

2. Methods

2.1. Glass and mineral standards

Haplobasaltic glasses were fused using high purity starting compounds of SiO_2, Al_2O_3, MgO and $CaCO_3$. 4 g of each sample was calcined for ~10 + h at ~1000 °C and then fused, at least twice, at ~100 °C above their liquidus. The glass chips were quenched by placing the bottom of the Pt crucible in room temperature water. The samples were hand ground between fusions under ethanol and placed in a drying oven at ~100 °C overnight before melting. Glass chips were analyzed by Raman spectroscopy to ensure that no crystals were present. Raman spectra of end member compositions are comparable to previous published spectra (Mysen et al., 1982; Matson et al., 1986). Mineral standards of the Ala Peidmont diopside ($Ca_{1.04}Mg_{0.92}Si_{2.00}O_6$) (sample M9109), Dog Lake diopside ($Ca_{1.03}Mg_{0.94}Si_{2.00}O_6$) (Ontario, Canada) (sample M42047), Vesuvius (Italy) anorthite ($Ca_{1.02}Al_{1.99}Si_{2.00}O_8$) (sample M11008), natural ($(Mg_{0.77}Zn_{0.02}\ Fe_{0.14})(Al_{1.91}Fe_{0.09})O_4$) (Notre-dame-du-Laus, Qué-bec) and synthetic ($(Mg_{0.37}Al_{0.42})Al_{2.00}O_4$) (aluminum-rich) spinel were used. Spinel standards were characterized by XRD to ensure purity. Both mineral standards and glasses were analyzed using electron microprobe (EMP) to determine their stoichiometry (Appendix A). Standards were used as a fingerprint reference to typical coordination environments.

2.2. XANES spectroscopy conditions

All XANES measurements were done at Canadian Light Source Inc. (CLS), Saskatoon, Canada at two beamlines: i) the variable line spacing-plane grating monochromator (VLS-PGM) (Si $L_{2,3}$- and Al $L_{3,2}$-edges) (Hu et al., 2007), and ii) the spherical grating monochromator (SGM) (Si, Al, Mg, and O *K*-edges and Ca $L_{2,3}$-edge) (Regier et al., 2007). Edge energies were internally calibrated between experimental sessions using SiO_2 polymorph standards (cristobalite, coesite, α-quartz), diopside, anorthite and/or spinel standards depending on the absorption edge. The energy resolution is ±0.05 eV or better for all XANES spectra. Analyses for mineral standards were carried out on powdered samples whereas thin glass chips were used for the haplobasaltic glass samples. The run conditions and calibration of the edge energies for various mineral standards are reported in Table 1. Spectra were simultaneously collected in both fluorescence yield (FY) and total electron yield (TEY) modes. TEY results were generally of poor quality for weakly conducting glasses therefore only FY yield spectra are reported below. FY spectra are known to sample a larger volume and therefore are more bulk sensitive (cf. Jiang and Spence, 2006; Schülke, 2007; Henderson et al., 2009, 2014). The SGM beamline at CLS was equipped with two (before December 2013) or four (after December 2013) silicon drift detectors (SDD). These detectors are positioned at a high angle to the incident beam to minimize self absorption. The SDDs allowed the absorption edge of interest to be isolated from minor contributions from edges of comparable energy. The largest interference, although still minor, was observed in the Ca $L_{2,3}$-edge data as the O *K*-edge lies only ~150 eV away. In addition, comparison between SDD data enabled erroneous diffraction peaks to be identified and removed. These anomalous diffraction peaks were observed in some of the mineral standards but not in the glass spectra. For a complete list of the peak positions in the XANES spectra see the compilation table in the Appendix B.

2.2.1. XANES *K*-edge and Ca $L_{2,3}$-edge data processing

After correcting each spectrum for anomalous diffraction peaks, the data were first normalized to the incident beam intensity (I_0) measured just before the sample chamber. Each spectrum then had a linear background fit to the pre-edge region removed. The data from each detector was then area normalized to one and summed. For each sample the spectrum reported is the average of 2–4 spectra. Each spectrum was then intensity normalized such that the L_2-edge intensity equaled one (e.g. Fig. 6b below).

2.2.2. Si $L_{2,3}$-edge data processing

The Si $L_{2,3}$-edge spectra were processed as follows: a) spectra were intensity normalized to the incoming intensity (I_0), recorded by a Ni mesh positioned upstream from the samples, b) the spectra were truncated to energies between 99 and 150 eV (Table 1) to avoid contributions from the Si L_1-edge, c) the background subtraction was done in two stages: i) the pre-edge background, defined between 95 eV and the first minimum (Table 2 below), was fit to a polynomial function in order to reduce its slope to approximately zero, ii) the edge background was removed by fitting a polynomial to the pre-edge minimum, the final intensity at 150 eV, and the minimum found between 118 eV to 125 eV depending on the spectrum of interest. Both the pre-edge